CNS Neuroscience & Therapeutics

ORIGINAL ARTICLE

CNS Neuroscience & Therapeutics

A New VMAT-2 Inhibitor NBI-641449 in the Treatment of Huntington Disease

Sheng Chen,[1,2] Xiao-Jie Zhang,[1] Wen-Jie Xie,[3] Hong-Yan Qiu,[1] Hui Liu[1] & Wei-Dong Le[1,4]

1 Institute of Neurology, Ruijin Hospital, Shanghai Jiaotong University School of Medicine, Shanghai, China
2 Department of Neurology, Baylor College of medicine, Houston, TX, USA
3 Diana Helis Henry Medical Research Foundation, New Orleans, LA, USA
4 Center for Translational Research of Neurology Diseases, The First Affiliated Hospital, Dalian Medical University, Dalian, China

Keywords
Endoplasmic reticulum stress; Huntington disease; NBI-641449; Therapeutics effects; VMAT-2 inhibitor.

Correspondence
W.-D. Le, M.D, Ph.D., Institute of Neurology, Ruijin Hospital, Shanghai Jiao Tong University School of Medicine, Shanghai 200025, China.
Tel.: +86-215-4669084;
Fax: +86-215-4669084;
E-mail: Wdle@sibs.ac.cn
Received 6 October 2014; revision 22 May 2015; accepted 24 May 2015

doi: 10.1111/cns.12425

The first two authors contributed equally to this work.

SUMMARY

Aims: To evaluate the effectiveness of a new VMAT-2 inhibitor NBI-641449 in controlling hyperkinetic movements of Huntington disease (HD) and to investigate its possible therapeutic effects. **Methods:** We applied three different doses of NBI-641449 (1, 10, 100 mg/kg/day) for 2 weeks in 4-month-old YAC128 mice and wild-type (WT) mice. Rotarod performance and locomotive activities were tested during the administration of the drug. The concentration of dopamine (DA) and its metabolites was quantified in the striatal tissues by high-performance liquid chromatography (HPLC). Neuron survival in striatum and huntingtin protein aggregates were assessed with immunostaining. Expression levels of endoplasmic reticulum (ER) stress proteins were detected by immunoblotting. **Results:** Rotarod performance was significantly improved after treatment with low or middle dose of NBI-641449 in YAC128 mice. Open field test showed that NBI-641449 treatment could attenuate the increased horizontal activity (HACTV), total vertical movement, moving time, and moving distance in YAC128 mice. High dose of NBI-641449 might cause sedative effects in WT and YAC128 mice. HPLC showed that NBI-641449 caused a dose-dependent decrease of DA, 3,4-dihydroxyphenylacetic acid, and homovanillic acid levels in the striatum. NeuN and DARPP-32 immunostaining revealed that NBI-641449 had no significant effect on the neuron survival in the striatum. However, NBI-641449 treatment reduced the huntingtin protein aggregates in the cortex of YAC128 mice. In addition, the levels of ER stress proteins were increased in YAC128 mice, which can be suppressed by NBI-641449. **Conclusions:** These findings suggest that this new VMAT-2 inhibitor NBI-641449 may have therapeutic potential for the treatment of HD.

Introduction

Huntington's disease (HD) is an autosomal dominant inherited neurodegenerative disorder caused by expansion of CAG triplet repeats in the huntingtin (*HTT*) gene and characterized by selective and progressive neuronal loss in the affected tissues, mostly in the striatum [1–3]. HD is typically diagnosed based on clinical features of movement symptoms, cognitive impairments, and psychological abnormality in the setting of a family history and can be confirmed by genetic testing [4,5]. There is currently no effective treatment to delay the onset of disease or slow the disease progression. A number of previous studies suggested that dopamine (DA) signaling pathway plays an important role in HD pathogenesis [6,7]. It is known that vesicular monoamine transporter-2 (VMAT-2) is a vital molecule in catecholamine storage and defect of it may cause neurodegeneration [8]. Several studies also reported that VMAT-2 inhibitor may benefit to HD treatment [9–11]. Tetrabenazine (TBZ) is a VMAT-2 inhibitor, which can cause depletion of DA content in the presynaptic vesicles and reduction in the dopaminergic tone. In previous clinical trials, TBZ showed some efficacy in relieving hyperkinetic movement in patients with HD [12–16]. Furthermore, it was demonstrated that long-term feeding with TBZ can alleviate the motor symptoms in YAC128 mouse model of HD and reduce the striatal neuron loss, which indicate its potential therapeutic effect for HD [17]. However, the underlying mechanisms of the therapeutic effects of TBZ on HD are largely unknown. Recently, Fuentes et al. [18] reported that inhibition of VMAT-2 can induce cell death in a substantia nigra (SN)-derived cell line, suggesting its potential neurotoxicity. This result poses question of safety for clinical use of VMAT-2 inhibitor. Recently, Neurocrine Inc. (San Diego, CA, USA) developed a new generation of VMAT2 inhibitor called NBI-641449, an analog of NBI-98854, which is undergoing a phase 3 clinical study for the treatment of hyperkinetic movement disorders. NBI-641449 can effectively regulate DA release but has minimal impact on the other monoamines (provided by Neurocrine Inc., unpublished data). The

selectivity may reduce the likelihood of "off target" side effects. Additionally, this novel agent has low, sustained, plasma and brain concentrations, which may minimize the potential side effects associated with excessive DA depletion (provided by Neurocrine Inc., unpublished data). This study is to evaluate the effectiveness of this drug in controlling abnormal motor symptoms of HD and to investigate whether it has neurotoxicity to neurons in nigro-striatal pathway. In addition, we attempt to test the biological effects of this new VMAT2 inhibitor in the brain of YAC128 mice, a transgenic animal model of HD [19].

The YAC128 mice express the full-length human *HTT* gene with 128 CAG repeats, whose phenotypes are similar to the patients with HD, which makes the transgenic mice as a unique model for the screening of novel therapeutic approaches for the treatment of HD [19–22]. In the YAC128 mice, hyperkinetic movement begins at 3 months of age with progressive motor impairment appearing at 6 months of age [21]. Significant decrease in striatal neuron survival usually starts from 12 months of age in the YAC128 mice [19]. Furthermore, the transgenic mice exhibit decreased brain weight and reduced striatal and cortical volumes at 9 months of age [19]. For the first step, we evaluate the antihyperkinetic effect and antineuron loss effect of NBI-641449 at early stage of the disease.

Although the mechanisms of HD remain unclear, endoplasmic reticulum stress (ER stress) may play an important role in this process [23]. Accumulation of intracellular protein aggregates may trigger ER stress as well as apoptosis, which can lead to cell death [23–25]. C/EBP homologous protein (CHOP), a key signaling protein of ER-stress-induced apoptosis, plays an essential role in ER stress [26]. Upregulating CHOP can trigger caspase 12 activation as well as inhibit Bcl-2 expression, which may induce apoptosis [27]. However, whether these factors are involved in HD neurodegeneration process remains largely unknown. In this study, we observed the possible anti-ER stress effects through inhibition of CHOP signal pathway. These experimental studies may provide more evidence for understanding mechanisms of VMAT-2 inhibitor in the treatment of HD.

Materials and Methods

Drug Delivery in Mice

YAC128 mice (FVBN/NJ background strain, No 004938) were obtained from Jackson Labs (Bar Harbor, ME, USA). Female YAC128 hemizygotous mice and age-matched wild-type (WT) littermates were used in all our experiments. NBI-641449 was obtained from Neurocrine Inc. prepared as low dose (1 mg/kg/day, NBI-1), middle dose (10 mg/kg/day, NBI-10), and high dose (100 mg/kg/day, NBI-100) in 50 μL of pure water. NBI-641449 was delivered to 4-month-old mice by oral feeding needle two times a day for two continuous weeks. WT mice were divided into four groups: WT control, WT-1 (treated with NBI-1), WT-2 (treated with NBI-10), and WT-3 (treated with NBI-100). YAC128 mice also were divided into four groups: YAC control, YAC-1 (treated with NBI-1), YAC-2 (treated with NBI-10), and YAC-3 (treated with NBI-100). All animal studies were approved by the Animal Ethics Committee of Baylor College of medicine and carried out in accordance with the Guidelines laid down by the NIH in the United States regarding the care and use of animals for experimental procedures (animal protocol 0014125).

Behavior Tests

Rotarod Performance

Rotarod performance was trained 1 day prior and tested in 2 weeks (2, 6, 10, 14 days) after the oral administration of NBI-641449. All the mice were trained on the rotarod rod for 120 second with three trials to get a baseline of performance. The rotarod assessments were performed using an accelerating rotarod treadmill (Columbus Instruments, Columbus, OH, USA) as previously described [6]. At each test point, mice were required to perch on the stationary rod for 30 second to adapt to the environment. Then the animals were trained at a constant speed of 5 rpm for 90 second. After this pretraining, mice were tested three times at 1-h intervals. During each test, the rotarod was set at a starting speed of 5 rpm for 30 second, and the speed was increased by 0.1 rpm/second. All animals were tested three times for each experiment, and the mean latency to fall off the rotarod recorded in the three trials was subjected to statistical analysis.

Open Field Analysis

Open field test, monitored by the AccuScan Digiscan system (AccuScan Instruments Inc., Columbus, OH, USA), was started 1 day prior and 2, 6, 10, and 14 days after the oral administration of NBI-641449. Four parameters collected by computer included: (1) horizontal activity (HACTV): the total number of beam interruptions in the horizontal sensor each 60 min; (2) vertical movement number: the total number of beam interruptions of the vertical sensors each 60 min; (3) total distance traveled: the distance traveled around the entire home cage in a continuous path (cm/60 min); and (4) total moving time: the total moving time in the entire home cage horizontally and vertically (second/60 min). The measurements were taken during the period between 9 AM and 11 AM in a dark room. Each mouse was placed in the testing chamber for 30 min for adaptation, followed by a 60 min recording by the computer-generated automatic analysis system.

Determination of Striatal DA, 3,4-Dihydroxyphenylacetic Acid, and Homovanillic Acid Levels

The concentration of DA was quantified in striatal tissues by HPLC, which is preformed as previously described [28,29]. Briefly, striatal tissues were homogenized (10% w/v) by sonication in ice-cold 0.1 M perchloric acid. Homogenates were centrifuged at 10,000 g for 10 min at 4°C, and the supernatants were collected and filtered through acro-disk filters (0.25 mL; Fisher Scientific, Pittsburgh, PA, USA) and subjected to HPLC (HTEC-500; Eicom, Kyoto, Japan) with the column (EICOMPAK SC-3ODS; Eicom) and detected by an electrochemical detector (AD Instruments Pty Ltd., Castle Hill, NSW, Australia). The mobile phase consisted of 0.1 mM citric acid, 0.1 M sodium acetate, 220 mg/L octane sulfate sodium, 5 mg/L EDTA, and 20% methanol, pH 3.5.

Immunoblotting Analysis

Total proteins were isolated from the tissues with RIPA lysis buffer containing 50 mM Tris-HCl (pH 7.4), 150 mM NaCl, 1% Nonidet P-40, 1 mM EDTA, 1 mM phenylmethylsulfonyl fluoride, and proteasome inhibitor cocktail. The protein concentrations were assayed from the resulting supernatants by the bicinchoninic acid assay (BCA) kit (Thermo Scientific, Waltham, MA, USA). Forty micrograms of proteins was loaded and separated on 8%, 10%, or 12% SDS–polyacrylamide gel electrophoresis (PAGE) gel. Proteins were transferred onto 0.45 or 0.22 μm PVDF membranes. Membranes were incubated in the presence of respective primary antibodies: CHOP (1:500; Cellsignal, Danvers, MA, USA), Bip (1:500; Cellsignal), and cleaved caspase-12 (1:500; Cellsignal). β-actin antibody (1:6000; Sigma, St. Louis, MO, USA) was used to equal protein loading. Peroxidase-conjugated secondary antibodies were used, and then protein bands were visualized using chemiluminescent horseradish peroxidase substrate (ECL; Pierce, Waltham, MA, USA) and quantified with an image analyzer (Image lab 4.1; Bio-Rad, Hercules, CA, USA).

Immunohistochemistry Staining for SN

The mice were terminally anesthetized and perfused transcardially with phosphate-buffered saline (PBS) and fixed with 4% paraformaldehyde. The brains were removed and postfixed in 4% paraformaldehyde at 4°C overnight and equilibrated in 15%/30% sucrose in PBS. The brains were sliced to 30-μm-thick coronal sections using a Leica sliding microtome (Leica 3050s, Wetzlar, Germany).

Serial frozen sections of the entire midbrain were systematically picked at 150-μm intervals and subjected to free-floating immunohistochemistry with rabbit antityrosine hydroxylase (TH, 1:1000; Millipore, Billerica, MA, USA) at 4°C overnight. The sections were washed in PBS and then incubated in the secondary antibody for 2 h at room temperature. For avidin–biotin–peroxidase method of TH-immunostaining, the secondary antibodies were biotinylated anti-rabbit IgG (1:200; Vector Laboratories, Burlingame, CA, USA), followed by avidin/biotin complex (ABC kit; Vector Laboratories) and 3, 3′-diaminobenzidine tetrachloride (DAB; Sigma) chromogen. For quantitative evaluation, the dissector technique was used to estimate the number of nigral neurons immunoreacted with TH antibody in animal midbrain. The number of neurons in a specific region was estimated by multiplying the total number of neurons counted in all section pairs by 5 to reflect the total number of sections from which the section pairs were chosen.

Assessment of Neuron Survival and Huntingtin Protein Aggregates in the Brain

The frozen brains were sliced to 30-μm-thick coronal sections spaced 360 μm. Slices of striatum were stained with NeuN monoclonal antibody (1:1000; Millipore) at 4°C overnight, which is present in most neurons, and DARPP-32 antibody (1:200; Proteintech, Chicago, IL, USA), which is a specific marker for medium spiny neurons in the striatum [30]. The second antibody was incubated for 2 h at room temperature. Quantitative analysis was preformed blindly to genotype and drug feeding. The grid size was set to 450 × 450 μm, and the counting frame was set to 50 × 50 μm. The neuropathological assessments were preformed as described previously [19].

For the detection of huntingtin aggregates, we used monoclonal EM48 antibody (1:100; Millipore) to stain the brain slices, which is specific for huntingtin aggregates [31]. Fluorescent dye Cy3-conjugated goat anti-mouse (Jackson ImmunoResearch, West Grove, PA, USA) was used as secondary antibody. Antifade reagent with 4′,6-diamidino-2-phenylindole (DAPI) was used to antifade the fluorescence and nuclear stain (Lifetechnologies, Waltham, MA, USA). Slices were visualized at 400× magnifications under a fluorescent microscope (Olympus, IX81, Tokyo, Japan).

Statistical Data Analysis

The data were analyzed using SPSS 17.0 (Chicago, IL, USA). The rotarod performance and open field test were analyzed using three-way analysis of variance (ANOVA) with repeated measures accounting for genotype, drug treatment, and time point. The data of EM48 aggregation were analyzed using one-way ANOVA followed by Tukey *post hoc* test. The other data were analyzed using two-way ANOVA followed by Tukey *post hoc* test. Significant differences were defined as $P < 0.05$. All values were presented as mean ± SEM.

Results

NBI-641449 Improves Rotarod Performance of YAC128 HD Mice

Basal rotarod performance for all groups was determined before initiation of drug feeding when the mice were 4 months of age

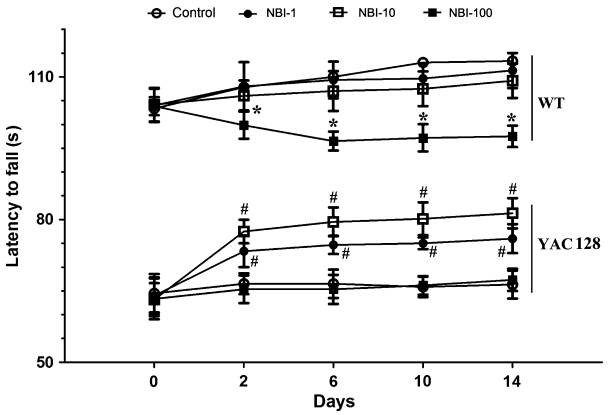

Figure 1 Rotarod performance of wild-type (WT) and YAC128 mice. An average latency to fall from the accelerating rotarod is shown for the WT mice and YAC128 mice in 4.5 months of age. The latency was significantly improved after NBI-641449 treatment with 1 and 10 mg/kg/day from 2 to 14 days. A total of 100 mg/kg/day group did not show significant improvement. A total of 1 and 10 mg/kg/day NBI-641449 treatment to WT mice had no apparent effects on the rotarod performance, while 100 mg/kg/day caused significant reduction compared to WT control mice at 2, 6, 10, and 14 days. N = 12 in each group. Values were shown as mean ± SEM. The results were analyzed using three-way ANOVA with repeated measures. $^{\#}P < 0.05$ when compared with YAC control; $^{*}P < 0.05$ when compared with WT control.

as described. The latency to fall from a rotating rod was used as a measurement of rotarod performance. Based on the results, we found all the WT mice performed better in rotarod assay than all the YAC128 mice (Figure 1). Feeding NBI-1 and NBI-10 to WT mice has no apparent effects on their rotarod performance from 2 to 14 days. However, NBI-100 treatment caused significant reduction of rotarod performance in 2, 6, 10, and 14 days when compared to WT control mice ($P < 0.05$) (Figure 1), which may be caused by the sedative effect of high dose of the agent. Furthermore, feeding NBI-1 and NBI-10 to YAC128 mice significantly improved their rotarod performance in 2, 6, 10, and 14 days when compared to YAC128 control mice ($P < 0.05$) (Figure 1). However, NBI-100 treatment had no apparent improvement in the period of 14 days rotarod test in YAC128 mice (Figure 1).

NBI-641449 Attenuates Abnormal Locomotor Activities of YAC128 HD Mice

As previously reported, YAC128 mice exhibit a hyperkinetic phenotype started from 3 months of age when compared with WT mice [19]. In our study, we found that when compared to YAC128 control mice, NBI-1-treated YAC128 mice showed significant decreased HACTV, total vertical movement, total distance traveled, and total moving time in 6, 10, and 14 days ($P < 0.05$) (Figure 2A–D). Feeding NBI-10 and NBI-100 to YAC128 mice significantly improved open field performance (reduced HACTV, total movement, total distance traveled, and total moving time) in 2, 6, 10, and 14 days when compared to YAC128 control mice ($P < 0.01$) (Figure 2A–D), which indicate that NBI-641449 can improve open field performance in a dose-dependent manner in YAC128 mice. Furthermore, NBI-1 and NBI-10 to WT mice did not show apparent difference in open field test, while NBI-100 to WT mice showed significant reduction in 6, 10, and 14 days when compared with WT control mice ($P < 0.05$, Figure 2A–D). These results further indicate possible sedative effect when treated with high dose of NBI-641449 in WT mice.

NBI-641449 Downregulates DA and its Metabolites in the Striatum

We used HPLC-electro-chemical detector to determine the concentrations of DA and its metabolites in the striatum of different groups of experimental mice. In the WT control mice, the mean levels of DA, 3,4-Dihydroxyphenylacetic Acid (DOPAC), and homovanillic acid (HVA) in the striatum were 82.0 ± 4.9, 28.0 ± 2.8, and 27.4 ± 3.3 ng/mg tissues (Figure 3A–C). The levels of DA and DOPAC in NBI-1-treated mice had no apparent

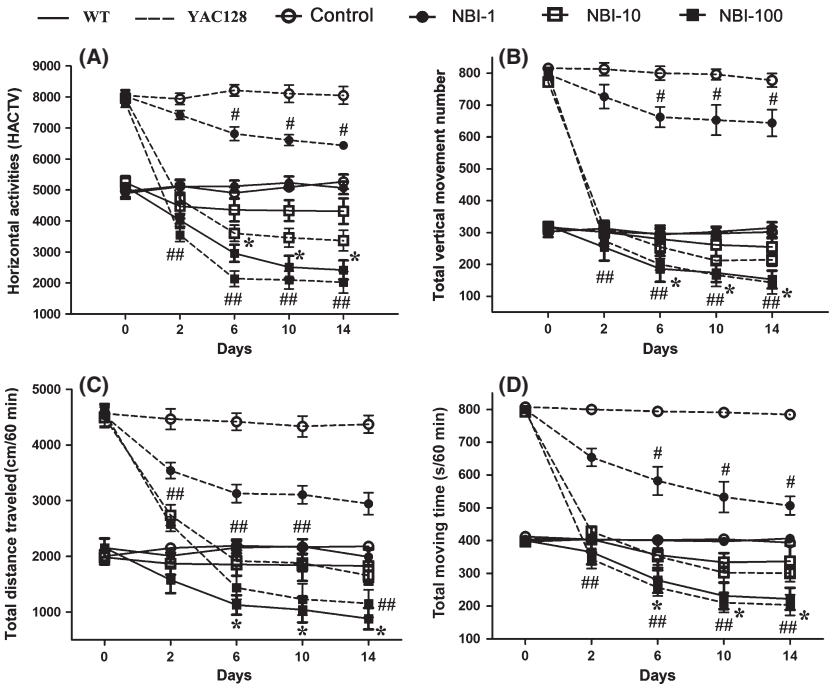

Figure 2 Open field test results of wild-type (WT) and YAC128 mice in 4.5 months of age. (**A**) horizontal activity (HACTV) = the total number of beam interruptions in the horizontal sensor each 60 min; (**B**) total vertical movement number = the total number of beam interruptions of the vertical sensors each 60 min; (**C**) total distance traveled = the distance traveled around the entire home cage in a continuous path (cm/60 min); and (**D**) total moving time = the total moving time in the entire home cage horizontally and vertically (second/60 min). The data for the WT mice were shown as full lines, while YAC128 mice as dotted lines. A total of 100 mg/kg/day NBI-641449 treatment significantly altered the open field performance in WT mice. A total of 10 and 100 mg/kg/day NBI-641449 treatment significantly improved the open field performance from 2 to 14 days when compared to YAC control mice. Feeding with 1 mg/kg/day NBI-641449 showed significant improvement of open field performance in 6, 10, and 14 days in YAC128 mice. N = 12 in each group. Values were shown as mean ± SEM. The results were analyzed using three-way ANOVA with repeated measures. $^{\#}P < 0.05$ and $^{\#\#}P < 0.01$ when compared with YAC control; $^{*}P < 0.05$ when compared with WT control.

difference when compared to WT control mice (Figure 3A,B), but the level of HVA in NBI-1-treated mice was reduced to 67.8% of WT control mice ($P < 0.05$) (Figure 3C). Furthermore, levels of DA, DOPAC, and HVA in NBI-10 and NBI-100-treated mice were significantly reduced when compared to WT control mice ($P < 0.01$) (Figure 3A–C). Similar to the effects of NBI-641449 in WT mice, we further found that NBI-641449 treatment at three doses resulted in downregulation of DA and its metabolites in the striatum in a dose-dependent manner (70.0 ± 7.9, 19.8 ± 4.9, 19.4 ± 3.2 ng/mg tissue for YAC-1 mice [NBI-1]; 41.4 ± 7.8, 14 ± 2.6, and 8.8 ± 3.7 ng/mg tissue for the YAC-2 [NBI-10] mice; and 19.1 ± 5.8, 7.0 ± 3.5, and 6.4 ± 2.3 ng/mg tissue for the YAC-3 mice [NBI-100]) (Figure 3A–C). These results suggest that inhibition of DA synthesis and metabolism by NBI-641449 may contribute to this anti-HD hyperkinetic effect in YAC128 mice.

NBI-641449 does not Alter the Number of TH-Positive Neurons in the SN of YAC128 Mice

To determine whether the DA neurons in the SN were affected in the YAC128 mice by NBI-641449 treatment, we used immunochemistry staining to detect TH-positive neurons in the SN in eight group mice. We found that there was no significant difference in the TH-positive neurons between all eight group mice (Figure S1A). Statistical analysis further suggested that there was no significant difference in TH-positive neurons between WT and YAC128 mice or NBI-641449-treated and untreated mice, which indicate that NBI-641449 may have no toxicity to DA neurons (Figure S1B).

NBI-641449 does not Significantly Affect the Neuron Survival in the Striatum of YAC128 Mice

Striatal cell loss is a defining neuropathological characteristic of HD [19]. To further assess the effect of NBI-641449 on the neuron survival in the striatum, we used immunostaining to detect the number of NeuN-positive cells in the striatum of different experimental mice. NeuN immunofluorescent staining revealed no obvious difference between eight groups of experimental mice (Figure S2A), which is consistent with the previous reports [6,19]. Quantitative analysis showed a 4.8% but not significant decrease in the number of striatal NeuN-positive neurons in YAC128 control mice as compared to WT control mice (Figure S2B, $P > 0.05$). Moreover, NBI-1 and NBI-10 treatment showed slight increase in the number of NeuN-positive neurons when compared to YAC128 control mice (Figure S2B, $P > 0.05$). There was no difference in the number of NeuN-positive neurons between NBI-100-treated YAC128 mice and YAC128 control mice (Figure S2B).

To further examine neuronal loss after the NBI-641449 treatment, the number of medium spiny neurons (MSNs) was assessed by immunostaining for DARPP-32, a protein specific to medium spiny neurons (MSNs) [30]. MSNs are considered as the most affected neurons in HD and also the major neuron type in the striatum [6]. Similar to the results of NeuN immunostaining, there was no apparent difference in all the eight groups of experimental mice (Figure 4A). Quantitative analysis indicated a 5.1% but not significant reduction in the number of DARPP-32-positive neurons in YAC128 control mice as compared to WT control mice (Figure 4B, $P > 0.05$). There was no significant difference between YAC control, YAC-1, YAC-2, and YAC-3 (Figure 4B,

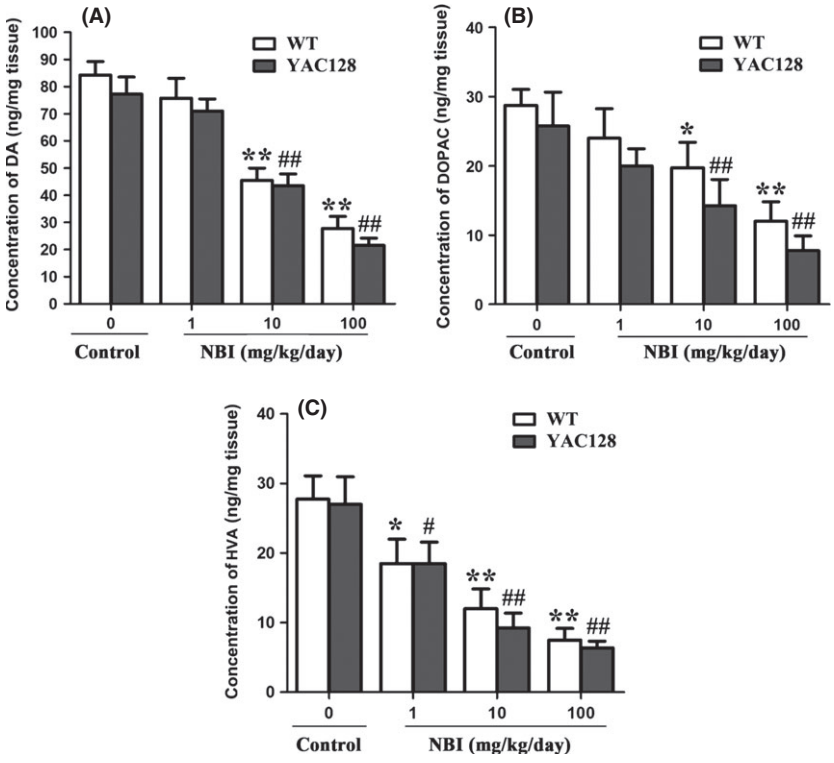

Figure 3 Levels of DA and its metabolites in striatum of wild-type (WT) and YAC128 mice in 4.5 months of age. (**A**) Concentration of DA in striatum area (ng/mg tissue); (**B**) concentration of DOPAC (ng/mg tissue); (**C**) concentration of HVA (ng/mg tissue). N = 4 in each group. Values were shown as mean ± SEM. The results were analyzed using two-way ANOVA followed by Tukey *post hoc* test. $^{**}P < 0.01$ and $^{*}P < 0.05$ when compared with WT control; $^{\#}P < 0.05$ and $^{\#\#}P < 0.01$ when compared with YAC control. HVA, homovanillic acid.

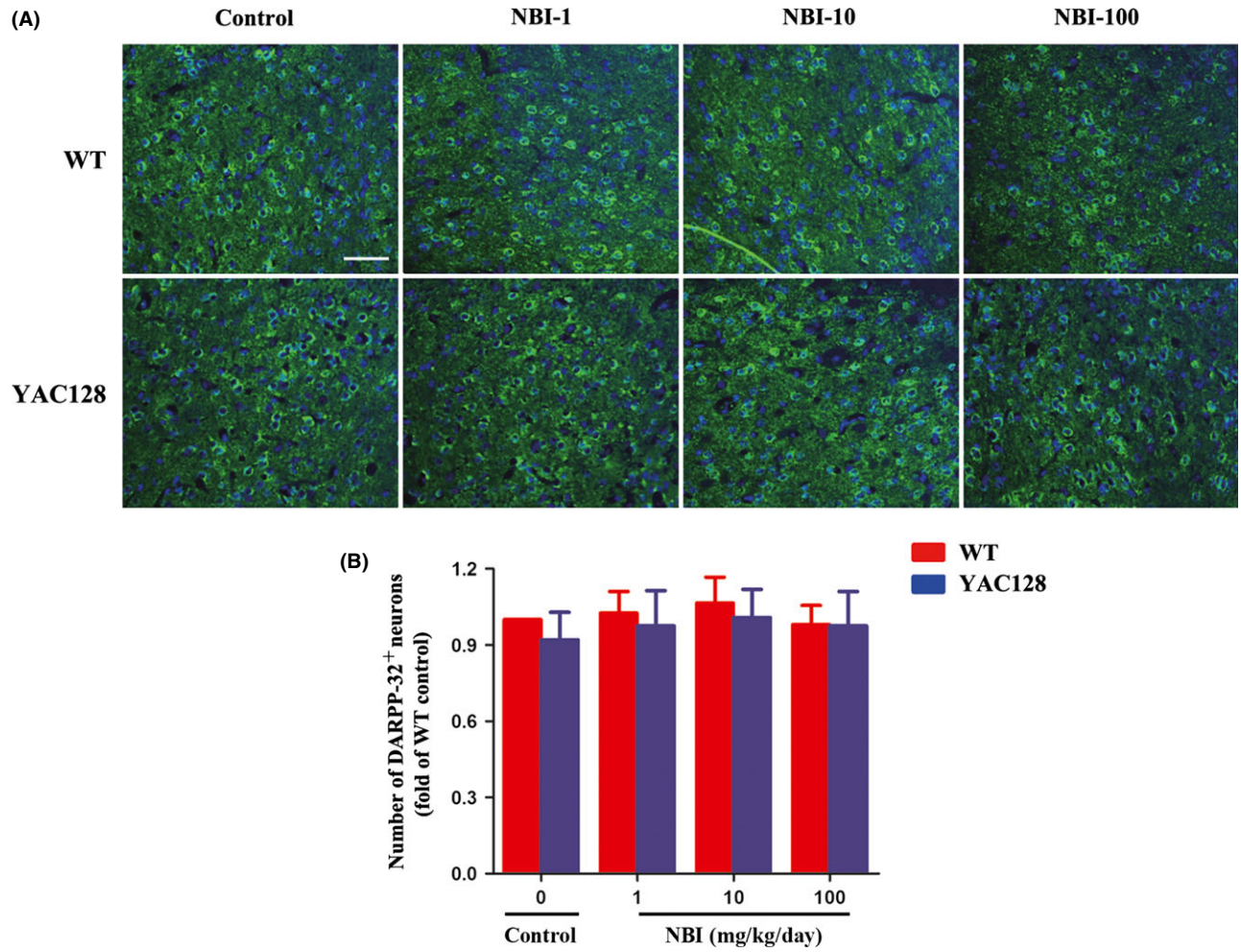

Figure 4 The survival of MSNs in wild-type (WT) and YAC128 mice. (**A**) Representative DARPP-32 staining of striatal sections from 4.5 months of age in WT and YAC128 mice; (**B**) the mean number of DARPP-32-positive neurons in striatum in eight different groups of mice. Nucleuses were marked with DAPI (blue). Statistical analysis showed that there was no significant difference in the numbers of DARPP-32-positive neurons in WT and YAC mice or NBI-641449-treated or untreated mice. N = 3 in each group. Values were shown as mean ± SEM. The results were analyzed using two-way ANOVA followed by Tukey *post hoc* test.

$P > 0.05$). These results indicate that NBI-641449 treatment has slight but not significant effect on the neuron survival in the striatum of YAC128 mice.

NBI-641449 Reduces Huntingtin Protein Aggregates in the Brain of YAC128 Mice

Brain sections from YAC128 were immune stained with EM48, an antibody that recognizes N-terminal huntingtin and is highly specific for aggregates [31]. Immunostaining revealed the obvious EM48-positive aggregates in the cortex of four groups YAC128 mice (Figure 5A), while no apparent EM48-positive aggregate was detected in the striatum of YAC128 mice (data not shown). Also, there was no obvious EM48-positive aggregate in the striatum or cortex in four groups of WT mice (Figure 5A). Furthermore, there was a significant reduction of EM48-positive aggregates in the cortex of NBI-641449-treated groups (NBI-1, NBI-10, NBI-100) as compared with YAC128 control mice (Figure 5A). Quantitative analysis showed that the density of EM48 immunostaining in cortex of NBI-1 mice was reduced to 60.4% of that observed in YAC128 control mice, while NBI-10 and NBI-100 mice were reduced to 42.5% and 47.6% of YAC128 control mice, respectively (Figure 5B). These results indicate that NBI-641449 can reduce the huntingtin protein aggregates in the cortex of YAC128 mice, which might involve in the therapeutic effects of NBI-641449 in HD mice.

NBI-641449 Reduces the Levels of ER Stress Proteins

Using immunoblotting, we further detected the levels of associated proteins in ER stress, including CHOP, Bip, and cleaved caspase-12 in the brain of 4.5 months of age in WT and YAC128 mice. Based on the results of behavior tests, we chose the middle

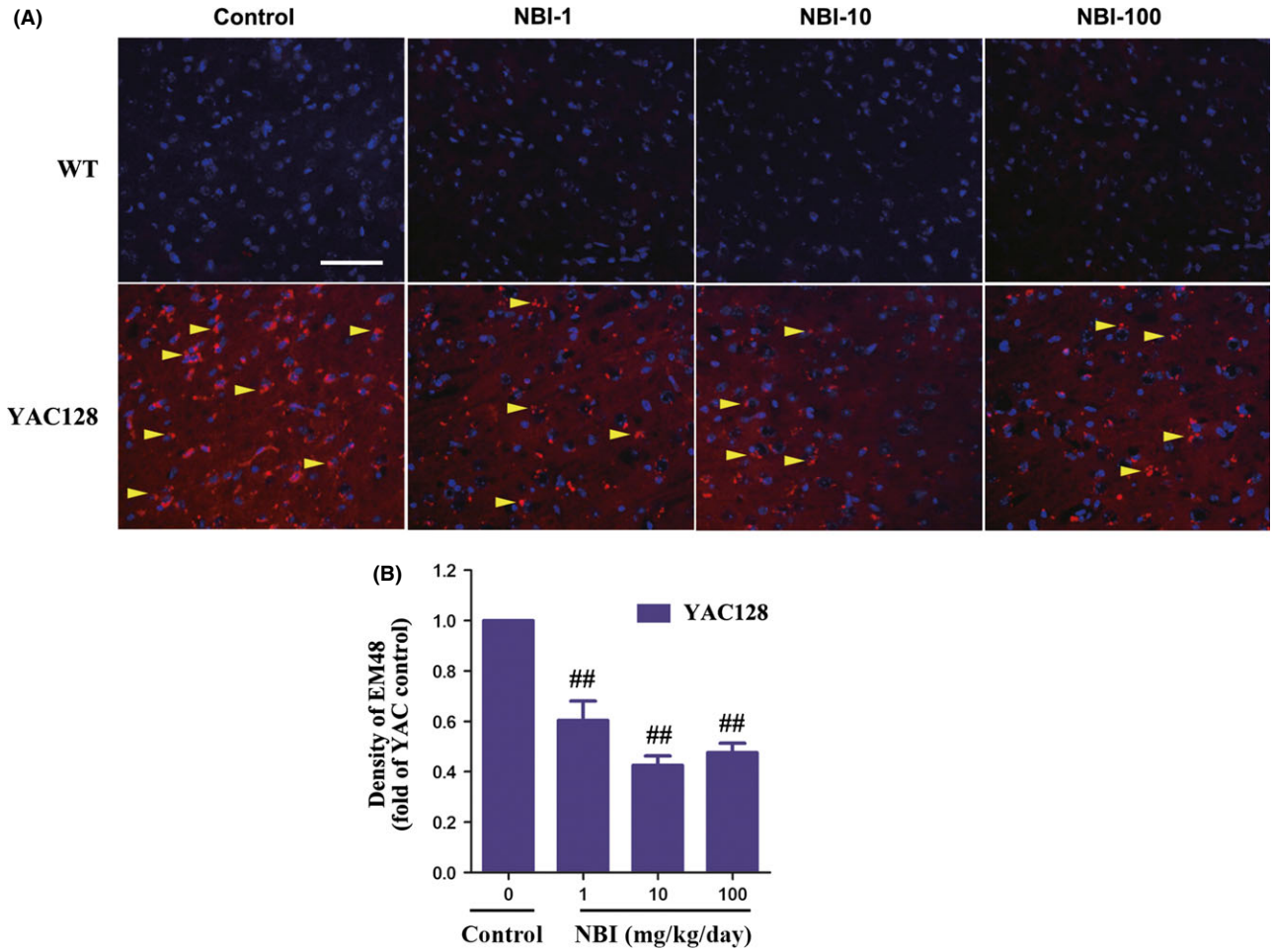

Figure 5 Huntingtin protein aggregates in cortex of wild-type (WT) and YAC128 mice. (**A**) Representative EM48-positive staining of cortical sections from WT and YAC128 mice in 4.5 months of age. Scale bar: 50 μm. Arrows indicate the huntingtin aggregates in cortex. Nucleuses were marked with DAPI (blue). (**B**) Quantitative analysis of EM48 density in the cortex of YAC128 mice. N = 3 in each group. Values were shown as mean ± SEM. The results were analyzed using one-way ANOVA followed by Tukey *post hoc* test. $^{\#\#}P < 0.01$ when compared with YAC control.

dose of 10 mg/kg/day to represent the effect of NBI-641449 in the ER stress in WT and YAC128 mice. The results of immunoblotting showed that the YAC128 mice had significantly high levels of ER-stress-associated proteins (CHOP, Bip, and cleaved caspase-12) as compared with WT mice (Figure 6A), while 10 mg/kg/day NBI-641449 treatment can significantly suppress the elevated levels of ER-stress-associated proteins in the YAC128 mice ($P < 0.01$) (Figure 6A). Statistics analysis further indicate that the levels of CHOP, Bip, and cleaved caspase-12 were reduced to 48.3%, 58.0%, and 51.5%, respectively, in NBI-10-treated YAC128 mice as compared to YAC128 control mice (Figure 6B). This result suggested that NBI-641449 has anti-ER stress effect in YAC128 mice.

Discussion

Although there is no effective therapy for HD, drugs aimed at controlling hyperactivity symptoms and delaying disease progression become research interests [1]. In our study, we found that NBI-641449, a new generation of VMAT-2 inhibitor, improved the behavior performance of YAC128 mice. Although NBI-641449 did not affect the number of DA neurons in SN area, application with this compound decreased the levels of DA and its metabolites in the striatum of the YAC128 mice. These findings suggest that therapies aimed toward inhibition of VMAT-2 are likely to have therapeutic benefits for the treatment of HD.

Inhibition of DA pathway is considered to be related with anti-hyperkinetic movement effect [6,19]. It has been reported that YAC128 mice impaired balance and motor function as shown in rotarod performance beginning at 3 months of age [17]. In our study, after treated with low and middle doses of NBI-641449, the latency to fall from the rod significantly prolonged, indicating that this drug may improve balance as well as motor function in YAC128 mice. However, the high dose NBI-641449 treatment in YAC128 mice fails to show improvement in rotarod performance, which might be explained by the drug's sedative effect at high dose. Rotarod performance of high dose NBI-641449 treatment in WT mice further indicated the possible sedative effect of this agent. Otherwise, we found that the hyperkinetic movements, tested by open field, in the HD mice were attenuated after the NBI-641449 treatment. These symptoms are similar with HD

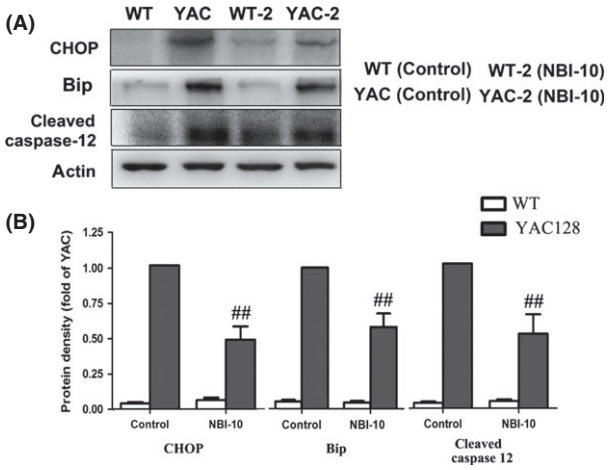

Figure 6 Levels of ER-stress-associated proteins in wild-type (WT) and YAC128 mice. (**A**) Western blot analysis of protein levels of CHOP, Bip, and cleaved caspase-12 in the WT control, WT-2 (NBI-10), YAC control, and YAC-2 (NBI-10) mice; (**B**) quantitative analysis of the ratio of CHOP, Bip, and cleaved caspase-12 in the four mouse groups. N = 3 in each group. Values were shown as mean ± SEM. The results were analyzed using two-way ANOVA followed by Tukey *post hoc* test. $^{\#\#}P < 0.01$ when compared with YAC control. ER, endoplasmic reticulum.

patients which are characterized by hyperactive chorea movement and mood instability at early stage of disease [1]. The anti-HD effects of NBI-641449 in the treatment of YAC128 mice may indicate its effects in controlling hyperactive symptoms in real patients with HD. In the future, more researches are needed to investigate whether this NBI-641449 has same therapeutic effects in the late stage of HD mice.

Tetrabenazine is the only FDA approved agent for the symptomatic management of HD, which binds to VMAT-2 to deplete monoamines and serotonin from presynaptic central nervous system neurons [32]. Previous clinical trials demonstrated that TBZ can efficiently reduce chorea symptoms in patients with HD compared with placebo group [12–16]. However, TBZ is not a specific DA depleting compound, other neurotransmitter innervations such as serotoninergic and some noradrenergic, which might lead to the side effects of depression, anxiety, parkinsonism, and so on [14,15]. NBI-641449 is a potent, highly selective VMAT-2 inhibitor which is designed to treat hyperkinetic movement disorders, including HD, tardive dyskinesia, dystonia, and others. Compared to TBZ, NBI-641449 has less impact on other monoamines, which might reduce the possibility of side effects during the treatment of HD. In our study, high dose of NBI-641449 to WT mice showed reduced hyperkinetic movements in open field test and significant reduction in rotarod test. These results further indicate the effect of NBI-641449 on a possible sedative effect that might occur at high dose but not at low and middle doses.

Striatal neuronal loss is one of the hallmarks of HD, and it was reported that the motor deficit in YAC128 mice is highly correlated with striatal neuronal loss [19]. MSNs are the major neuronal cell type in striatum and also the most affected neurons in the disease progression of HD [33]. Previous studies reported that the significant change of neuronal density in the striatum and the loss of striatal volume usually started from 9 months of age in the YAC128 mice [19]. In our study, we found about 4.8% and 5.1% but not significant reduction of NeuN-positive and DARPP-2-positive neurons, respectively, in the striatum of 4.5 months old YAC128 mice, which is consistent with the previous studies [19]. Furthermore, based on our results, we found the motor defects in 4 months of age in YAC128 mice, and low and middle doses of NBI-641449 can improve the behavior performance in YAC128 mice. We speculate that the improvement of behavior performance might not be caused by the change of neuron survival in the striatum or SN, rather than the functional alteration of MSNs or other neurons in YAC128 mice.

Intercellular aggregate of mutant huntingtin protein is considered as one of hallmarks for the pathological feature of HD [34]. Immunostaining revealed that the circular, densely stained intraneuronal aggregates were located in the striatum, cerebral cortex, cerebellum, and the spinal cord in HD [35,36]. EM48, an antibody against the N-terminal of huntingtin, appears to be more sensitive for the huntingtin aggregates in the brain of HD mouse model or patients [31]. Previous study demonstrated that EM48-positive aggregates were more prone to locate in cortex than in striatum. In patients with HD, cytoplasmic aggregates are much more common than nuclear aggregates in presymptomatic stage [31]. Further evidence supported that no apparent EM48-positive inclusions were observed in striatal cells of YAC128 mice until 18-month-olds [19]. In our study, consistent with previous studies, we found EM48-positive aggregates appeared in the cytoplasm of cortical neurons, not in the striatal cells of 4.5-month-old YAC128 mice. Indeed, there is controversy in the literature about the connection between huntingtin aggregates in cerebral cortex and the neuronal dysfunction in the striatum. One possibility is that the majority of neurons in the striatum are projection neurons, and striatal pathology could exist by the potential importance of glutamatergic corticostriatal projections in HD [37]. Besides, strategies for reducing huntingtin aggregates have been proved beneficial in HD mouse models, which further indicated the neurotoxicity from the huntingtin aggregates [38]. In our study, three doses of NBI-641449 can significantly reduce the EM48-positive aggregates in cerebral cortex, which might be involved in its anti-HD effects in YAC128 mice.

Accumulating evidence indicated that cytoplasmic/nuclear hungtingtin aggregation may generate chronic ER stress which leads to neuronal dysfunction in HD [39]. Further study reported that N-terminal mutant huntingtin proteins activated cellular pathways linked to ER stress causing cell death, and inhibition of ER stress increased cell survival [40]. Prolonged ER stress can activate CHOP expression, a key signaling protein of ER-stress-induced apoptosis [23,41]. CHOP-induced apoptosis can be suppressed by the pro-survival protein Bcl-2 that regulates cross talk between the ER and mitochondria [41]. In addition, CHOP activation could also upregulate caspase 12, which is located in the ER and is responsible for ER-stress-induced apoptosis [41,42]. In our study, we found that after treatment of NBI-641449, the expression levels of ER-stress-related proteins CHOP, Bip, and cleaved caspase-12 were downregulated, which highly suggest that NBI-641449 may have therapeutic effects mediated by anti-ER stress in YAC128 mice.

Until now, no treatment can alter the disease course of HD, and numerous experiments in animal model and clinic trials in patients are undergoing to lessen symptoms of movement and rescue the neurons degeneration [43]. Besides TBZ, atypical antipsychotic, olanzapine, got encouraging responses from small open-label studies [44]. A novel dopaminergic stabilizer, pridopidine, acts as a modulator of D_2 receptor activity in central nervous system, which has been recently developed for treatment of movement and psychiatric disorders including HD [45]. Other RNAi therapy targeting mutant huntingtin protein or stem cell transplant therapy has been initiated in cell and animal models, before conducting clinic trials in patients [1].

Conclusion

Despite advances have been made in understanding the pathology of HD, there remains no specific therapeutic drugs for this devastating disease. It is clear in the present study that a new VMAT-2 inhibitor, NBI-641449, has efficacy of controlling hyperkinetic symptom of HD with little toxicity to neuron survival in striatum. In addition, feeding this agent significantly reduces the hungtingtin protein aggregates in cerebral cortex in YAC128 mice and shows anti-ER stress effect through its inhibition on CHOP, Bip, and cleaved caspase-12 pathways. These results provide further molecular evidence that NBI-641449 possesses potential anti-HD property, which may warrant further clinical study in patients with HD to determine whether the drug can slow down the disease progression.

Acknowledgments

This work was funded by a research grant from the Chinese National Sciences Foundation (NO. 81430021 and 81370470), PhD Innovation Fund of Shanghai Jiaotong University School of Medicine (BXJ 201218) and PhD Tutor Fund of Chinese Ministry of Education (20120073110077).

Conflict of Interest

The authors declare no conflict of interest.

References

1. Imarisio S, Carmichael J, Korolchuk V, et al. Huntington's disease: From pathology and genetics to potential therapies. *Biochem J* 2008;**412**:191–209.
2. Ross CA, Tabrizi SJ. Huntington's disease: From molecular pathogenesis to clinical treatment. *Lancet Neurol* 2011;**10**:83–98.
3. Gusella JF, MacDonald ME. Huntington's disease: Seeing the pathogenic process through a genetic lens. *Trends Biochem Sci* 2006;**31**:533–540.
4. Li SH, Li XJ. Huntingtin–protein interactions and the pathogenesis of Huntington's disease. *Trends Genet* 2004;**20**:146–154.
5. Reiner A, Dragatsis I, Dietrich P. Genetics and neuropathology of Huntington's disease. *Int Rev Neurobiol* 2011;**98**:325–372.
6. Tang TS, Chen X, Liu J, Bezprozvanny I. Dopaminergic signaling and striatal neurodegeneration in Huntington's disease. *J Neurosci* 2007;**27**:7899–7910.
7. Walker FO. Huntington's disease. *Lancet* 2007;**369**:220.
8. Caudle WM, Richardson JR, Wang MZ, et al. Reduced vesicular storage of dopamine causes progressive nigrostriatal neurodegeneration. *J Neurosci* 2007;**27**:8138–8148.
9. Gros Y, Schuldiner S. Directed evolution reveals hidden properties of VMAT, a neurotransmitter transporter. *J Biol Chem* 2010;**285**:5076–5084.
10. Staal RG, Hogan KA, Liang CL, German DC, Sonsalla PK. In vitro studies of striatal vesicles containing of the vesicular monoamine transporter (VMAT2): Rat versus mouse differences in sequestration of 1-methyl-4-phenylpyridinium. *J Pharmacol Exp Ther* 2000;**293**:329–335.
11. Zheng G, Dwoskin LP, Crooks PA. Vesicular monoamine transporter 2: Role as a novel target for drug development. *AAPS J* 2006;**8**:E682–E692.
12. Fasano A, Cadeddu F, Guidubaldi A, et al. The long-term effect of tetrabenazine in the management of Huntington disease. *Clin Neuropharmacol* 2008;**31**:313–318.
13. Frank S. Tetrabenazine: The first approved drug for the treatment of chorea in US patients with Huntington disease. *Neuropsychiatr Dis Treat* 2010;**6**:657–665.
14. Huntington Study Group. Tetrabenazine as antichorea therapy in Huntington disease: A randomized controlled trial. *Neurology* 2006;**66**:366–372.
15. Kenney C, Jankovic J. Tetrabenazine in the treatment of hyperkinetic movement disorders. *Expert Rev Neurother* 2006;**6**:7–17.
16. Le W, Rowe D, Xie WJ, Ortiz I, He Y, Appel SH. Microglial activation and dopaminergic cell injury: An in vitro model relevant to Parkinson's disease. *J Neurosci* 2001;**21**:8447–8455.
17. Wang H, Chen X, Li Y, Tang TS, Bezprozvanny I. Tetrabenazine is neuroprotective in Huntington's disease mice. *Mol Neurodegener* 2010;**5**:18.
18. Fuentes P, Paris I, Nassif M, Caviedes P, Segura-Aguilar J. Inhibition of VMAT-2 and DT-diaphorase induce cell death in a substantia nigra-derived cell line–an experimental cell model for dopamine toxicity studies. *Chem Res Toxicol* 2007;**20**:776–783.
19. Slow EJ, van Raamsdonk J, Rogers D, et al. Selective striatal neuronal loss in a YAC128 mouse model of Huntington disease. *Hum Mol Genet* 2003;**12**:1555–1567.
20. Graham RK, Slow EJ, Deng Y, et al. Levels of mutant huntingtin influence the phenotypic severity of Huntington disease in YAC128 mouse models. *Neurobiol Dis* 2006;**21**:444–455.
21. Menalled L, El-Khodor BF, Patry M, et al. Systematic behavioral evaluation of Huntington's disease transgenic and knock-in mouse models. *Neurobiol Dis* 2009;**35**:319–336.
22. Dey ND, Bombard MC, Roland BP, et al. Genetically engineered mesenchymal stem cells reduce behavioral deficits in the YAC128 mouse model of Huntington's disease. *Behav Brain Res* 2010;**214**:193–200.
23. Vidal RL, Hetz C. Crosstalk between the UPR and autophagy pathway contributes to handling cellular stress in neurodegenerative disease. *Autophagy* 2012;**8**:970–972.
24. Pan T, Kondo S, Le W, Jankovic J. The role of autophagy-lysosome pathway in neurodegeneration associated with Parkinson's disease. *Brain* 2008;**131**:1969–1978.
25. Zhang X, Chen S, Song L, et al. MTOR-independent, autophagic enhancer trehalose prolongs motor neuron survival and ameliorates the autophagic flux defect in a mouse model of amyotrophic lateral sclerosis. *Autophagy* 2014;**10**:588–602.
26. Jin ML, Park SY, Kim YH, Oh JI, Lee SJ, Park G. The neuroprotective effects of cordycepin inhibit glutamate-induced oxidative and ER stress-associated apoptosis in hippocampal HT22 cells. *Neurotoxicology* 2014;**41**:102–111.
27. Liu D, Zhang M, Yin H. Signaling pathways involved in endoplasmic reticulum stress-induced neuronal apoptosis. *Int J Neurosci* 2013;**123**:155–162.
28. Li X, Yang D, Li L, Peng C, Chen S, Le W. Proteasome inhibitor lactacystin disturbs the intracellular calcium homeostasis of dopamine neurons in ventral mesencephalic cultures. *Neurochem Int* 2007;**50**:959–965.
29. Du Y, Li X, Yang D, et al. Multiple molecular pathways are involved in the neuroprotection of GDNF against proteasome inhibitor induced dopamine neuron degeneration in vivo. *Exp Biol Med (Maywood)* 2008;**233**:881–890.
30. Ouimet CC, Langley-Guillon KC, Greengard P. Quantitative immunocytochemistry of DARPP-32-expressing neurons in the rat caudatoputamen. *Brain Res* 1998;**808**:8–12.
31. Gutekunst CA, Li SH, Yi H, et al. Nuclear and neuropil aggregates in Huntington's disease: Relationship to neuropathology. *J Neurosci* 1999;**19**:2522–2534.
32. Hayden MR, Leavitt BR, Yasothan U, Kirkpatrick P. Tetrabenazine. *Nat Rev Drug Discov* 2009;**8**:17–18.
33. Vonsattel JP, Myers RH, Stevens TJ, Ferrante RJ, Bird ED, Richardson EP. Neuropathological classification of Huntington's disease. *J Neuropathol Exp Neurol* 1985;**44**:559–577.
34. Montserrat A, Steven F. Protein aggregates in Huntington's disease. *Exp Neurol* 2012;**238**:1–11.
35. Davies SW, Scherzinger E. Nuclear inclusions in Huntington's disease. *Trends Cell Biol* 1997;**7**:422.
36. Becher MW, Kotzuk JA, Sharp AH, et al. Intranuclear neuronal inclusions in Huntington's disease and dentatorubral and pallidoluysian atrophy: Correlation between the density of inclusions and IT15 CAG triplet repeat length. *Neurobiol Dis* 1998;**4**:387–397.
37. Sapp EG, Aizawa H, Bird E, et al. Evidence for a preferential loss of enkephalin immunoreactivity in the external globus pallidus in low grade Huntington's disease using high resolution image analysis. *Neuroscience* 1995;**64**:397–404.
38. Zhang X, Smith DL, Meriin AB, et al. A potent small molecule inhibits polyglutamine aggregation in Huntington's disease neurons and suppresses neurodegeneration in vivo. *Proc Natl Acad Sci U. S. A* 2005;**102**:892–897.
39. Matus S, Glimcher LH, Hetz C. Protein folding stress in neurodegenerative diseases: A glimpse into the ER. *Curr Opin Cell Biol* 2011;**23**:239–252.

40. Reijonen S, Putkonen N, Norremolle A, Lindholm D, Korhonen L. Inhibition of endoplasmic reticulum stress counteracts neuronal cell death and protein aggregation caused by N-terminal mutant huntingtin proteins. *Exp Cell Res* 2008;**314**:950–960.
41. Chen S, Zhang X, Yang D, et al. D2/D3 receptor agonist ropinirole protects dopaminergic cell line against rotenone-induced apoptosis through inhibition of caspase- and JNK-dependent pathways. *FEBS Lett* 2008;**582**: 603–610.
42. Zhang K, Kaufman RJ. The unfolded protein response: A stress signaling pathway critical for health and disease. *Neurology* 2006;**66**:S102–S109.
43. Aleksandar V. Treatment of Huntington disease. *Curr Treat Options Neurol* 2013;**15**:424–438.
44. Bonelli RM, Mahnert FA, Niederwieser G. Olanzapine for Huntington's disease: An open label study. *Clin Neuropharmacol* 2002;**25**:263–265.
45. Waters S, Ponten H, Klamer D, Waters N. Co-administration of the dopaminergic stabilizer pridopidine and tetrabenazine in rats. *J Huntingtons Dis* 2014;**3**:285–298.

Supporting Information

The following supplementary material is available for this article:

Figure S1. The number of TH-positive neurons in the SN of WT and YAC128 mice.

Figure S2. Neuropathological analysis of WT and YAC128 mice.